Critical Behavior and Lack of Self Averaging in the Dynamics of the Random Potts Model in Two Dimensions

C. Deroulers
Laboratoire de Physique Théorique de l'École Normale Supérieure, 24 rue Lhomond, 75231 Paris Cedex 05, France[*]

A. P. Young
Department of Physics, University of California, Santa Cruz CA 95064, USA and Department of Theoretical Physics, 1 Keble Road, Oxford OX1 3NP, England[†]

(Dated: February 8, 2002)

We study the dynamics of the q-state random bond Potts ferromagnet on the square lattice at its critical point by Monte Carlo simulations with single spin-flip dynamics. We concentrate on $q = 3$ and $q = 24$ and find, in both cases, conventional, rather than activated, dynamics. We also look at the *distribution* of relaxation times among different samples, finding different results for the two q values. For $q = 3$ the relative variance of the relaxation time τ at the critical point is finite. However, for $q = 24$ this appears to diverge in the thermodynamic limit and it is $\ln\tau$ which has a finite relative variance. We speculate that this difference occurs because the transition of the corresponding pure system is second order for $q = 3$ but first order for $q = 24$.

PACS numbers: PACS numbers: 75.40.Cx, 75.50.Lk, 05.50.+q, 75.40.Mg

I. INTRODUCTION

The random q-state Potts model[1] in two-dimensions has recently been the subject of extensive study. One reason for this interest is that disorder even changes the *order* of the transition for $q > 4$, where it is first order in the pure case but must be continuous[2–4] in two-dimensions for all-q. Another reason interest is the prediction by Ludwig[5], later confirmed by numerical simulations[6–8], of multi-fractal exponents at the critical point. Although there has been a lot of numerical work on the static critical exponents[6–14], there has been less on the dynamics, though there have been some recent studies based on the "short-time dynamics"[15–17] approach. Here we perform a careful analysis of the dynamics of the Potts model in two dimensions by Monte Carlo simulations. Our motivation is two-fold:

Firstly, Cardy[18] has raised the possibility that, at least for certain types of dynamics, one might have *activated* dynamical scaling, in which the log of the characteristic time τ (i.e. the barrier height) varies with a power of an appropriate length scale l i.e. $\ln\tau \sim l^\psi$ where ψ is the "barrier" exponent. This is in contrast to *conventional* dynamical scaling in which τ itself varies with a power of l. i.e. $\tau \sim l^z$, where z is the dynamical exponent. Activated dynamics has been proposed by Fisher[19] for the random field Ising model where the fixed point (of the renormalization group) is at $T = 0$. First order transitions can also be described by a $T = 0$ fixed point and also have activated dynamics. In that case the barrier exponent ψ is equal to $d-1$ for a discrete broken symmetry, where d is the dimension, so $\psi = 1$ here.

We study two values of q: $q = 3$ where the pure system has a second order transition and so activated dynamics seems unlikely for the random case, and $q = 24$ where the pure system has a first order transition so there is a greater possibility that the random problem will have activated dynamics. The size of the first order jump increases as q gets large, and we find that we need $q \geq 16$ to clearly see activated dynamics for the *pure* system for the range of sizes studied. Hence, for the *random* case, we take a rather large number of Potts states, $q = 24$, since activated dynamics is easily seen in this case for the pure system, so we feel we have a good chance of seeing it in the random case too, if it occurs. In fact, we find conventional dynamical scaling for both values of q, but, as we shall discuss, have some concern as whether this is the true asymptotic behavior for $q = 24$.

Secondly, there has recently been considerable discussion about lack of self averaging for static quantities in random systems at the critical point. It is found[20–22] that if disorder is irrelevant, then the relative variance, R_X, of a static quantity X tends to zero in the thermodynamic limit like $L^{\alpha/\nu}$, where L is the lattice size, and α (< 0) and ν are the specific heat and correlation length exponents, respectively. This is called weak self averaging. However, if disorder is relevant then R_X tends to a universal constant, indicating lack of self-averaging. In this paper we consider the question of self averaging for *dynamics*, which has not been discussed before, to our knowledge. Disorder is relevant for both values of q that we study, and yet we find rather different distributions of the relaxation time τ in the two cases. For $q = 3$ we find a finite relative variance for τ but, perhaps surprisingly, for $q = 24$ this appears to diverge in the thermodynamic limit and it is $\ln\tau$ which has a finite relative variance.

Sec. II describes the model and the quantities we calculate. Results for the pure models are given in Sec. III while results for the random system are given in Sec. IV. Our conclusions are summarized in Sec. V.

II. THE MODEL

The Hamiltonian of the q-state Potts model is given by

$$\beta\mathcal{H} = -\sum_{\langle i,j\rangle} K_{ij}\delta_{n_i n_j}, \tag{1}$$

where each site i on an $N = L \times L$ square lattice is in one of q-states, characterized by an integer $n_i = 1, 2, \cdots, q$. The couplings, K_{ij}, are positive, and include the factor of $\beta \equiv 1/k_B T$. They are independent random variables, drawn from a probability distribution, $P(K)$.

For the pure case, the system is at criticality if the "dual coupling" K^*, defined by[1,23]

$$(e^K - 1)(e^{K^*} - 1) = q, \tag{2}$$

is equal to K, i.e. $K^* = K = K_c$, where $e^{K_c} = 1 + \sqrt{q}$. For the random case it is possible to choose a self-dual *distribution* of the couplings to ensure that the system is at the critical point. We take the distribution suggested by Olson and Young[8] (OY) since this is both very broad (so the system is far from the pure fixed point), and also does not have a substantial weight near $K = 0$ (so the system is far from the percolation fixed point). In terms of $x \equiv e^{-K}$, the OY distribution is[24]

$$P_X(x) = \frac{2}{\pi}\,\frac{\sqrt{q}}{(1-x)^2 + qx^2}. \tag{3}$$

To generate random numbers with probability $P_X(x)$ one takes x to be

$$x = \frac{1}{1 + \sqrt{q}\tan(\pi r/2)}, \tag{4}$$

where r is a random number with a uniform distribution between 0 and 1.

We focus on the time dependent magnetization squared, defined by

$$m(t)^2 = \frac{q}{q-1}\left(\sum_{n=1}^{q}\rho_n(t)^2 - \frac{1}{q}\right), \tag{5}$$

where $\rho_n(t)$ is the fraction of sites in state n at time t, The initial configuration is completely random and so $m(t)^2$ increases, eventually reaching its equilibrium value for $t \to \infty$. Note that $m(t)^2$ is invariant under global symmetry transformations which permute the states n. Particularly useful is the average value of $m(t)^2$ normalized by its equilibrium value $m(\infty)^2$, i.e.

$$\widehat{m}(t)^2 = \frac{[\langle m(t)^2\rangle]_{\mathrm{av}}}{[\langle m(\infty)^2\rangle]_{\mathrm{av}}}, \tag{6}$$

where $[\cdots]_{\mathrm{av}}$ denotes an average over disorder, and $\langle\cdots\rangle$ denotes a thermal average. Clearly $\widehat{m}(0)^2 \simeq 0$ (for finite-N it is $O(1/N)$), and $\lim_{t\to\infty}\widehat{m}(t)^2 = 1$.

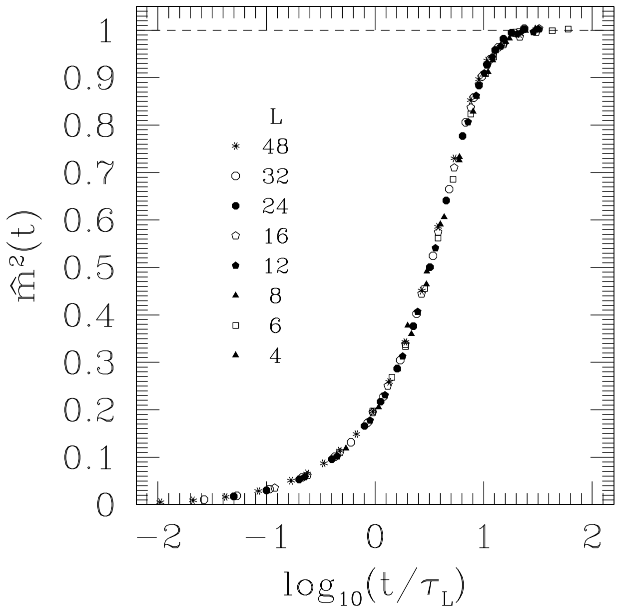

FIG. 1: Results for $\widehat{m}(t)^2$, defined in Eqs. (6) and (5), for the pure system for $q = 3$. The horizontal axis t/τ_L, where τ_L is determined for each lattice size by requiring that the data collapse. Results for the τ_L are shown in Fig. 2.

In addition to results for the *average* decay of the magnetization, we also discuss the *distribution* of relaxation times of the total magnetization.

Since we want to use a realistic form for the dynamics, we use standard Monte Carlo methods rather than one of the more efficient cluster algorithms[25,26] that reduce critical slowing down. However, we did use the Wolff[26] algorithm to obtain more accurate estimates for some of the equilibrium values of m^2, needed in the denominator of Eq. (6).

III. RESULTS FOR THE PURE SYSTEM

The transition is second order for $q < 4$, so we expect conventional dynamical scaling in this region. To see this we show in Fig. 1 data for $\widehat{m}(t)^2$ for $q = 3$ against $\ln(t/\tau_L)$, where τ_L is chosen for each L in order to collapse the data. A log-log plot of τ_L against L is shown in Fig. 2, which demonstrates nice power-law scaling. A fit, omitting the $L = 4$ data point, gives a dynamical exponent $z = 2.18 \pm 0.04$. An activated scaling plot of $\ln\tau_L$ against L^ψ does not work unless ψ is chosen to be extremely small, in which case this is equivalent to a conventional scaling plot.

By contrast, for $q > 4$ the transition is first order which leads to activated scaling with $\psi = 1$, as discussed in Sec. I. The correlation length at the critical point has been computed in Ref. 28 and we show a table of results,

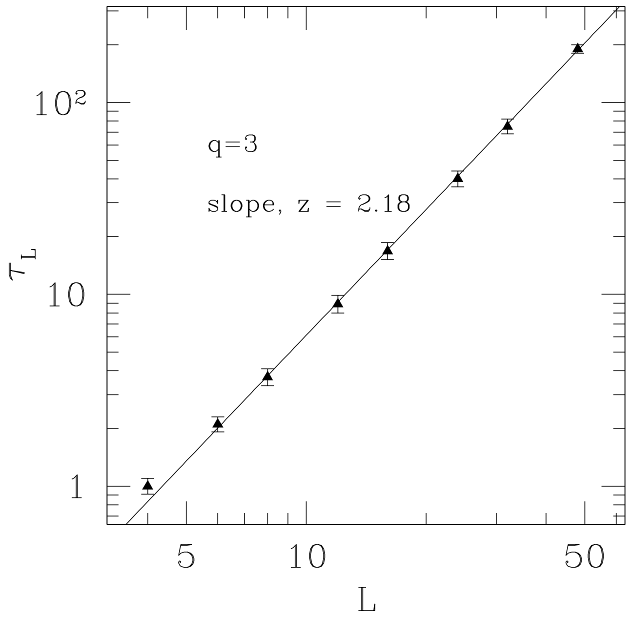

FIG. 2: Results for τ_L for the pure system for $q = 3$, determined so that the data in Fig. 1 collapse. Since all the τ_L can be multiplied by the same constant with no effect on the quality of the data collapse, we arbitrarily set $\tau_4 = 1$. The best fit, omitting the $L = 4$ point, gives $z = 2.18 \pm 0.04$.

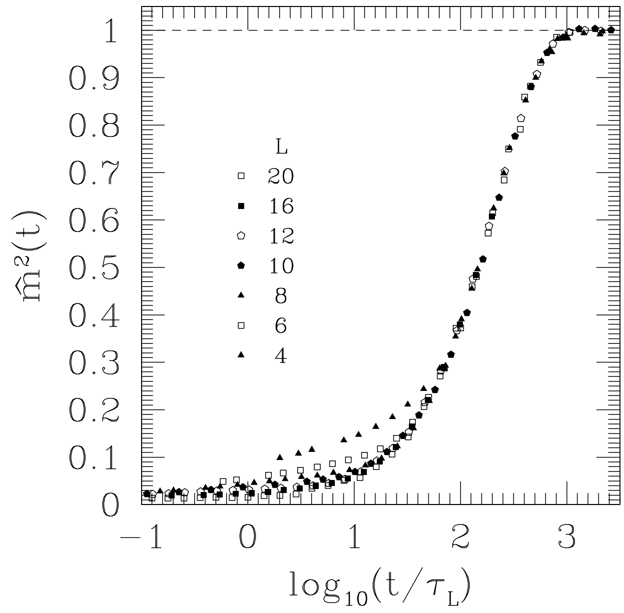

FIG. 3: Results for $\widehat{m}(t)^2$ for the pure system for $q = 24$. The horizontal axis t/τ_L, where τ_L is determined for each lattice size by requiring that the data collapses as well as possible. The resulting values for the τ_L are plotted in Figs. 4 and 5.

q	$\xi_{\rm crit}$
4	∞
5	2512
6	158.9
8	23.88
12	6.548
16	3.746
24	2.155
32	1.608

TABLE I: The values of the correlation length at the critical point of the pure system for certain values of q. These results are obtained from expressions in Ref. 28.

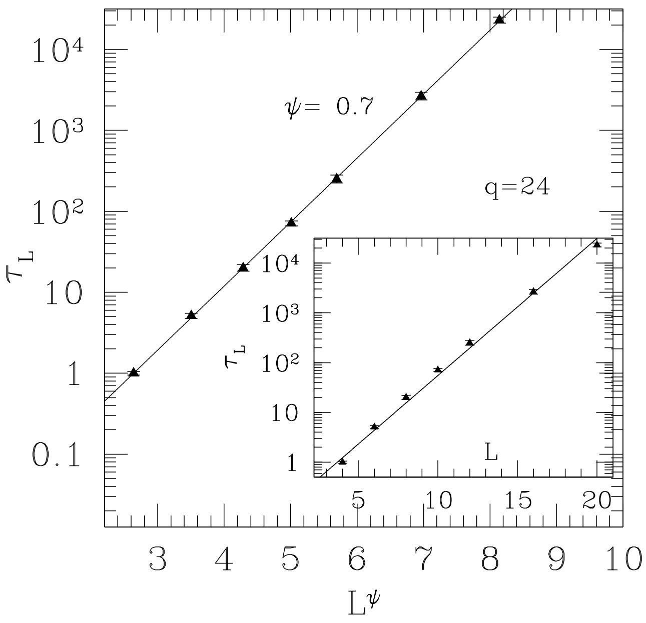

FIG. 4: A plot of τ_L (on a log scale) against L^ψ for the pure system for $q = 24$. The data fits a straight line well, indicating activated scaling, though fitting gives $\psi = 0.7 \pm 0.1$, rather than the asymptotic value of 1. The inset shows a plot assuming $\psi = 1$. Distinct curvature indicates a less good fit as discussed in the text.

computed from the expressions in this reference, for certain values of q in Table I. In order to see the first order nature of the transition in numerical simulations the sizes studied must be larger than the critical correlation length which suggests that we should take $q \geq 16$.

Data for $q = 24$ for $\widehat{m}(t)^2$ is shown in Fig. 3. The data collapse is good except for very short times, which is presumably not in the scaling regime. Interestingly, the data for $q = 3$ in Fig. 1, does scale even at very short times.

Activated and conventional scaling plots for $q = 24$ are shown in Figs. 4 and 5 respectively. The activated scaling

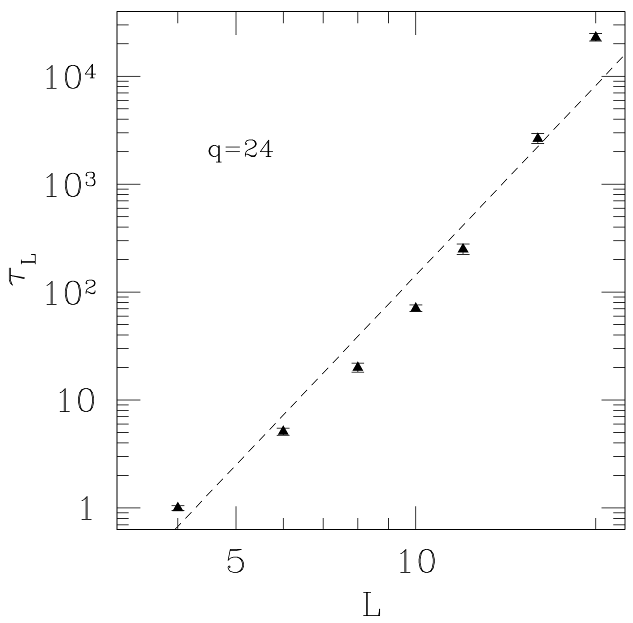

FIG. 5: A log-log plot of τ_L against L for the pure system for $q = 24$. The data shows pronounced curvature, indicating that conventional dynamical scaling does not work.

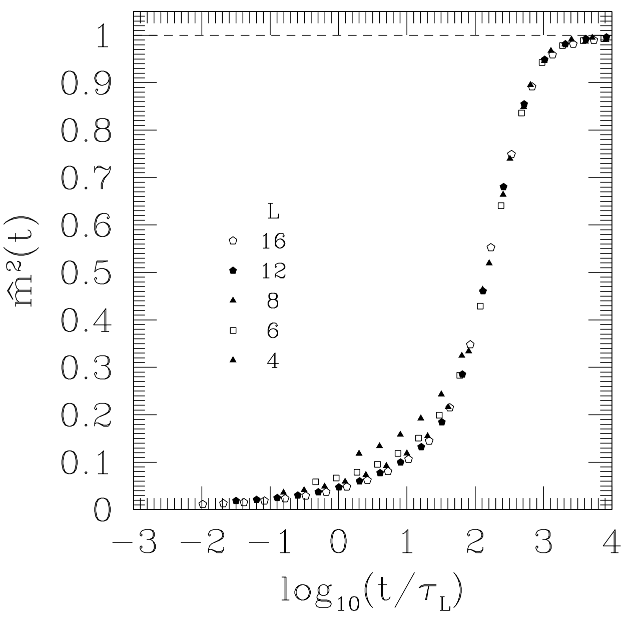

FIG. 6: Results for $\widehat{m}(t)^2$ for the random system with the Olson-Young distribution, Eq. (3), for $q = 24$. The horizontal axis t/τ_L, where τ_L is determined for each lattice size by requiring that the data collapses as well as possible. Results for the τ_L are shown in Figs. 7 and 8.

fit works well, but with a barrier exponent $\psi \simeq 0.7 \pm 0.1$, rather than the expected value of 1. The inset shows the data plotted with $\psi = 1$. The fit has a probability (Q-factor) of 6.1×10^{-12}, which is very low, whereas the fit with $\psi = 0.7$ has a Q-factor of 0.92, which is good. Presumably the value $\psi = 0.7$ is only an effective exponent which fits the data for the range of sizes studied, since one expects to see $\psi = 1$ for sufficiently large sizes. As shown in Table I, the correlation length at criticality decreases with increasing q so one expects to be closer to the asymptotic value of ψ at large q for the modest range of sizes that we can simulate. Our results are consistent with this since we find effective values of ψ equal to $0.55, 0.7$ and 0.9 for $q = 16, 24$ and 32, respectively. For $q = 8$, activated scaling only worked for ψ around 0.1 or less, which is sufficiently small that it is not significantly different from conventional scaling. Thus, although one expects activated scaling asymptotically for $q = 8$, one is far from this regime for the range of sizes that we can study. This is not surprising since the the correlation length at criticality, shown in Table I, is about 24 lattice spacings. Recently, Özoğuz et al.[27] have studied the dynamics of the pure Potts model at criticality for $q = 6$ and 7. By using the Wolff[26] algorithm, they are able to study larger sizes than us, and they also incorporate corrections to finite size scaling. In this way, they find that their results are consistent with activated scaling with $\psi = 1$.

The main conclusion from this section is that activated dynamics is only seen easily in the *pure* model for $q \geq 16$. To determine if the *random* model has activated dynamics, we expect that one should choose q to be *larger* than the value where it can be seen for the pure system, i.e. we need $q > 16$.

IV. RESULTS FOR THE RANDOM SYSTEM

A. Dynamics of the averaged order parameter

Data for $\widehat{m}(t)^2$ for the random system with the Olson-Young distribution, Eq. (3), for $q = 24$ is shown in Fig. 6. The relaxation times, τ_L have been determined by requiring that the data for large times collapses, (with τ_4 arbitrarily set to unity), and are shown on a log-log plot in Fig 7. The fit is good and the slope gives the dynamical exponent,

$$z = 3.76 \pm 0.04 \qquad (q = 24). \tag{7}$$

We have also attempted to scale the data using activated dynamical scaling. However, we find only satisfactory fits are for ψ very small, see Fig. 8, which are not significantly different from the power law fit in Fig. 7. The inset shows a plot with a larger value of ψ, 0.7. The large curvature shows that this does not work.

It appears, then, that the random Potts model has conventional dynamical scaling. However, when we discuss distributions of relaxations times in Sec. IV B we shall

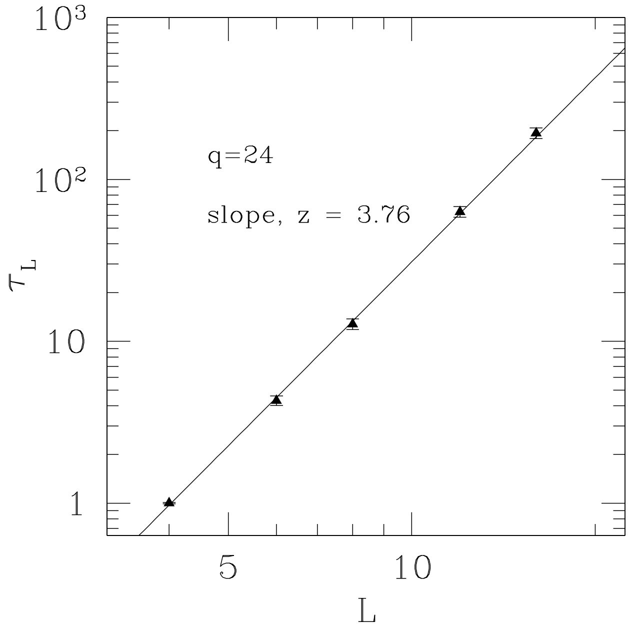

FIG. 7: A log-log plot of τ_L against L for the random system with the Olson-Young distribution, for $q = 24$. The straight line fit works well and gives a slope of $z = 3.76 \pm 0.04$.

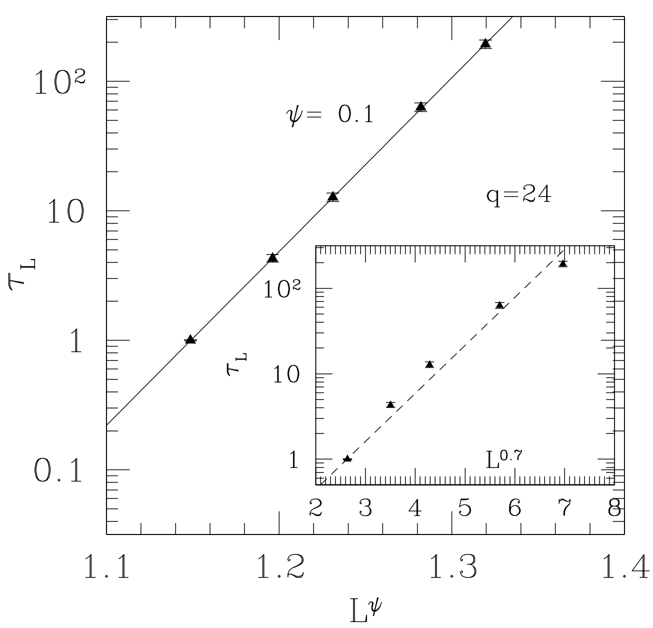

FIG. 8: An activated scaling plot of τ_L for the random system with the Olson-Young distribution, for $q = 24$. The only fits which work well have very small ψ, $\psi = 0.1$ is shown here, which, for the range of sizes studied, is not significantly different from the power law fit shown in Fig. 7. The inset shows a plot with $\psi = 0.7$, which is the best value for the pure system, see Fig. 4, but which clearly doesn't work for the random case because of the pronounced curvature.

see that the situation is rather more complicated, and the true asymptotic behavior is perhaps not clear.

We have also investigated the case of $q = 3$, which is unlikely to have activated dynamical scaling, since the pure system has a continuous transition, and indeed we find that conventional scaling works well, see Fig. 9. The fit gives

$$z = 3.24 \pm 0.03 \qquad (q = 3). \tag{8}$$

From Eqs. (7) and (8) it appears that z increases with increasing q and so our results are compatible with the value 3.41 ± 0.06 obtained by Pan et al.[16] for $q = 8$.

B. Distribution of relaxation times

Since disorder is relevant for all q greater than two, it is expected[20–22] that static quantities are not self-averaging at the critical point. Presumably dynamical quantities like the relaxation time are also not self-averaging but this does not seem to have been much discussed up to now. We have therefore also studied the *distribution* of relaxation times for the $q = 3$ and $q = 24$ Potts models. For each realization of the disorder (i.e. *sample*), we generate the time dependent squared magnetization, normalized by the equilibrium value for that sample (which we get with a good precision thanks to the Wolff algorithm), i.e.

$$\widetilde{m}(t)^2 = \frac{\langle m(t)^2 \rangle}{\langle m(\infty)^2 \rangle}. \tag{9}$$

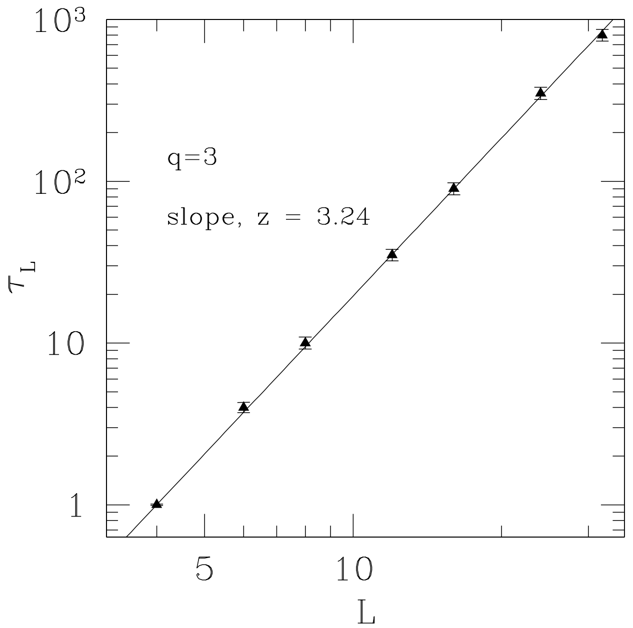

FIG. 9: A log-log plot of τ_L against L for the random system with the Olson-Young distribution, for $q = 3$. The straight line fit works well and gives a slope of $z = 3.24 \pm 0.03$.

q	L	samples
3	4	2241
3	6	1600
3	8	1537
3	12	105
24	4	2739
24	6	2223
24	8	868
24	12	1012

TABLE II: Parameters of the simulations used to study the distribution of relaxation times for the OY distribution for different values of q and lattice size L.

The thermal average is obtained by repeating the simulation 10^4 times with the same random bonds but starting from different initially disordered spin configurations.

We find that the *shape* of $\widetilde{m}(t)^2$ is strongly sample-dependent. We have tried various definitions to determine a relaxation time τ for a single sample: the time necessary for $\widetilde{m}(t)^2$ to reach a fixed value (0.3, 0.4, 0.5, 0.6, 0.7, 0.8 and 0.9) and the "integrated time" defined by $\int_0^\infty (1-\widetilde{m}^2(t))dt$. We checked that all these times, yield the same scaling behavior. The best choice, which minimizes the error bars, is the time to reach 0.60, which will be used from now on.

We have investigated the distribution of relaxation times for $q = 3$ and 24. However, since we need to repeat the dynamical evolution many times (10^4 in practice), and since we need to repeat this for many samples, the range of sizes that we could study is rather restricted, $L \leq 12$. The number of samples used for the different sizes and q values is given in table Table II.

Fig. 10 shows data for the *cumulative* distribution of τ for $q = 3$ for different sizes with a logarithmic horizontal scale. One sees that the distributions for different sizes are shifted horizontally but otherwise look very similar. This is confirmed by Fig. 11 in which the values for τ are scaled by the average relaxation time for each size. The data collapses moderately well, indicating that $\tau/[\tau]_{\rm av}$ has a (non-trivial) distribution which is independent of size, and which is presumably also universal. Hence all powers of moments of the form $[\tau^n]_{\rm av}^{1/n}$, (and the corresponding cumulants) all vary with L in the same way as the mean, i.e. as L^z. In particular, the relative variance,

$$R_\tau = \frac{[\tau^2]_{\rm av} - [\tau]_{\rm av}^2}{[\tau]_{\rm av}^2}, \qquad (10)$$

is a constant for $L \to \infty$ for $q = 3$. This is analogous to the lack of self-averaging in *static* quantities at the critical point which has been discussed before[20–22]. Note that the distribution of $\ln\tau/[\ln\tau]_{\rm av}$ is sharp at large L, i.e. $\ln\tau/[\ln\tau]_{\rm av}$ is self-averaging. We show the sharpening of the distribution of $\ln\tau/[\ln\tau]_{\rm av}$ in Fig. 12.

The average relaxation time, $[\tau]_{\rm av}$, defined in this sub-

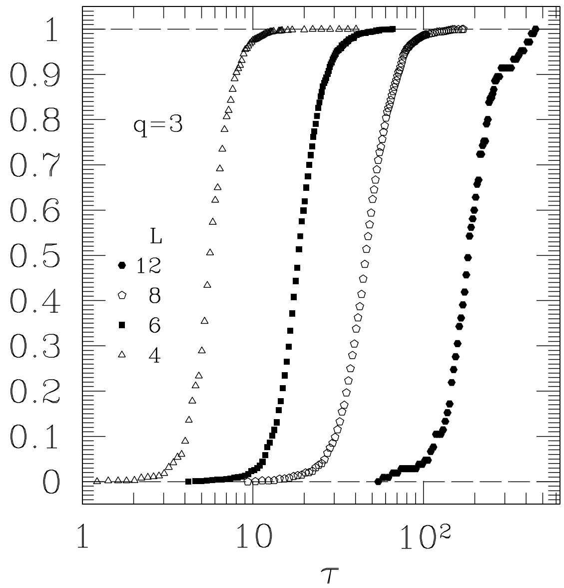

FIG. 10: Cumulative distribution functions of τ for the Olson-Young distribution of random bonds, $q = 3$.

section is not precisely the same as the relaxation time τ_L defined in terms of the dynamics of the square of the average magnetization in Sec. IV A. However, one expects that they should be proportional to each other, and indeed this the case since a fit of $\ln[\tau]_{\rm av}$ against $\ln L$ gives a slope of $z = 3.39 \pm 0.10$, essentially in agreement with Eq. (8).

Fig. 13 shows data for the cumulative distribution of τ for $q = 24$. In contrast to the data for $q = 3$ in Fig. 10, the curves for larger sizes are not only shifted to the right but also become broader. Hence the data does not collapse in a plot of $\tau/[\tau]_{\rm av}$ as shown in Fig. 14. However, if we consider the distribution of the *logarithm* of τ then a plot of $\ln\tau/[\ln\tau]_{\rm av}$ does scale, as shown in Fig. 15. Hence for $q = 24$, we find that R_τ diverges for $L \to \infty$, whereas $R_{\ln\tau}$ is finite, where $R_{\ln\tau}$ is defined in a similar way to R_τ in Eq. (10). Hence for $q = 24$, but not $q = 3$, one can say that is is the *barriers* which have a finite relative variance.

Since we have seen that $\ln\tau$ is the appropriate scaling variable for $q = 24$ we need to see how the average of this quantity varies with size. In Fig. 16 we show a plot of $[\ln\tau]_{\rm av}$ against $\ln L$, which works quite well with a slope 3.60 ± 0.09. If we define, possibly different, exponents z_n by $[\tau^n]_{\rm av}^{1/n} \sim L^{z_n}$ then the slope in Fig. 16 is z_0. Since $[\ln\tau]_{\rm av} \sim \ln L$ we have conventional, rather than activated, dynamics because in the latter case one would have $[\ln\tau]_{\rm av} \sim L^\psi$. This is also what we found in Sec. IV A. However, since we now see that the scaling variable is is $\ln\tau$ rather than τ, we need to discuss further the behavior of averages of powers of τ. We shall

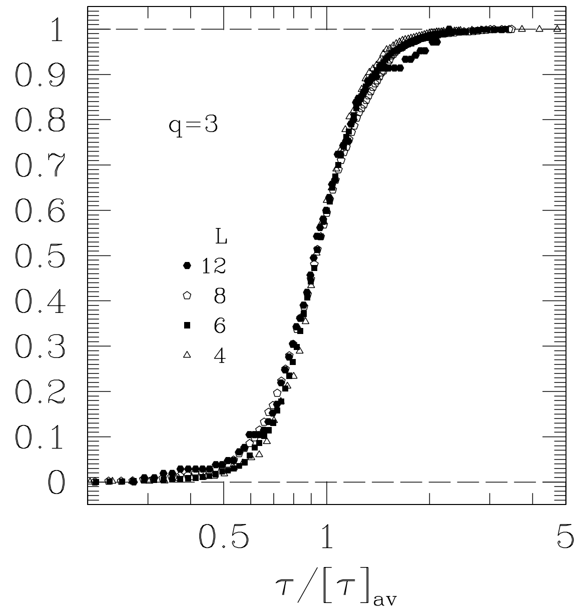

FIG. 11: Cumulative distribution functions of $\tau/[\tau]_{\rm av}$ for the Olson-Young distribution of random bonds, $q = 3$. This rescaling works

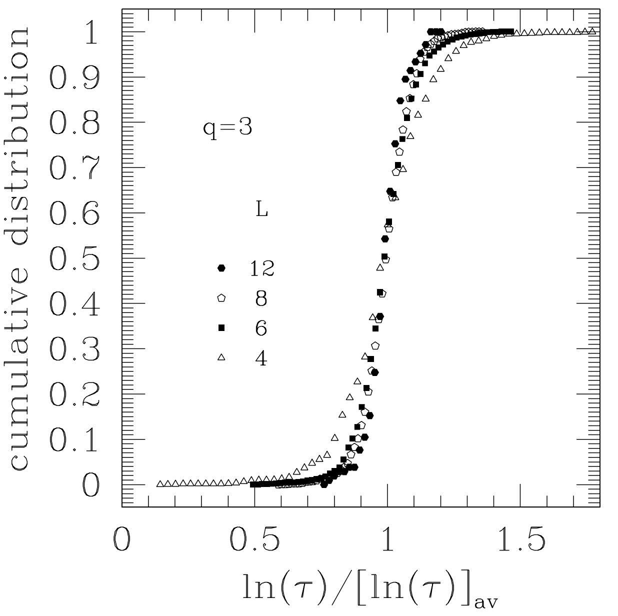

FIG. 12: Cumulative distribution functions of $\ln\tau/[\ln\tau]_{\rm av}$ for the Olson-Young distribution of random bonds, $q = 3$. This rescaling doesn't work since the distribution get narrower for larger L.

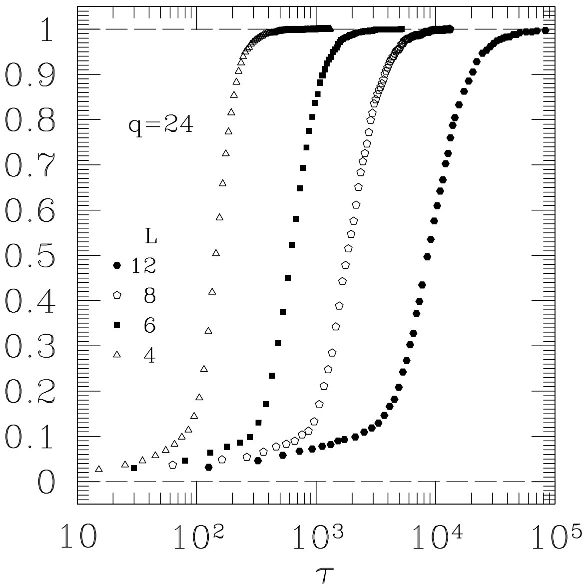

FIG. 13: Cumulative distribution functions of τ for the Olson-Young distribution of random bonds, $q = 24$.

see that this additional analysis implies that the results in Sec. IV A for $q = 24$ may not describe the asymptotic behavior for large L.

Because $\ln\tau$ is the scaling variable, we can write

$$
\begin{aligned}
[\tau^n]_{\rm av} &= [e^{n\ln\tau}]_{\rm av} \\
&= \int e^{n\ln\tau} f\left(\frac{\ln\tau}{[\ln\tau]_{\rm av}}\right)\frac{d\ln\tau}{[\ln\tau]_{\rm av}} \\
&= \int e^{nx[\ln\tau]_{\rm av}} f(x)\,dx \\
&= \int e^{nx(a+z_0\ln L)} f(x)\,dx, \qquad (11)
\end{aligned}
$$

where $f(x)$ is the scaling function for $x \equiv \ln\tau/[\ln\tau]_{\rm av}$, and the last equality has used the fit shown in Fig. 16.

From Eq. (11) we see that the behavior of $[\tau^n]_{\rm av}$ for large L depends on the form of the scaling function $f(x)$ for large x. If there is a very sharp cutoff at $x^\star$ say, then the integral is dominated by values in the vicinity of the cutoff and so $[\tau^n]_{\rm av} \sim e^{nx^\star(a+z_0\ln L)} \sim L^{nx^\star z_0}$, which gives $z_n = x^\star z_0$, independent of n, for $n > 0$. This is conventional dynamical scaling, except that the value of z_0 is different from that of z_n with $n > 0$. However, more generally, $[\tau^n]_{\rm av}^{1/n}$ would not vary as L^{z_n}, and hence would not correspond to conventional dynamical scaling. For example, a Gaussian form for $f(x)$ would give $[\tau^n]_{\rm av} \sim \exp(\text{const. } (\ln L)^2)$, which increases with L faster than than any power but is slower than exponential. This behavior is in between conventional and activated dynamics.

We have tried to estimate the behavior of $[\tau^n]_{\rm av}$ for

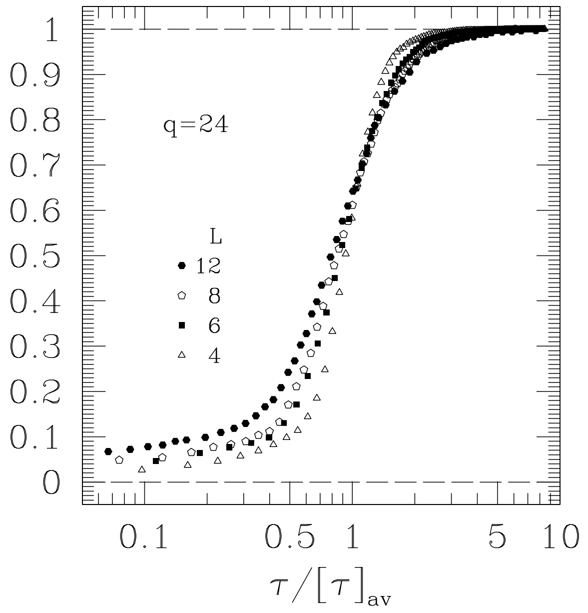

FIG. 14: Cumulative distribution functions of $\tau/[\tau]_{\rm av}$ for the Olson-Young distribution of random bonds, $q = 24$. This rescaling doesn't work.

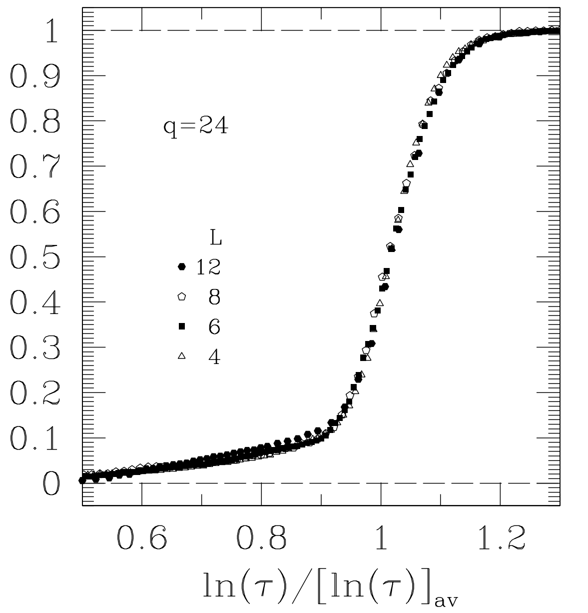

FIG. 15: Cumulative distribution functions of $\ln\tau/[\ln\tau]_{\rm av}$ for the Olson-Young distribution of random bonds, $q = 24$. This rescaling works, except for the shortest times.

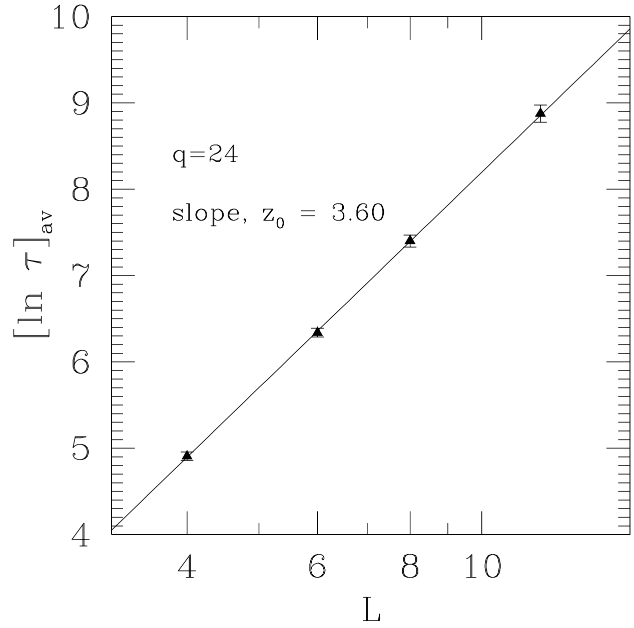

FIG. 16: A plot of $[\ln\tau]_{\rm av}$ against $\ln L$, which gives a slope of $z_0 = 3.60$.

large L by noting that

$$[\tau^n]_{\rm av} = g(-in[\ln\tau]_{\rm av}), \tag{12}$$

where

$$g(k) = \int_0^\infty e^{ikx} f(x)\, dx, \tag{13}$$

is the Fourier transform of the scaling function $f(x)$. Since $f(x)$ is normalized and has mean unity by definition, we can write

$$g(k) = \exp(ik + u(k)), \tag{14}$$

where

$$u(k) = \sum_{n=2}^{\infty} \frac{\langle x^n\rangle_c (ik)^n}{n!}, \tag{15}$$

in which $\langle x^n\rangle_c$ denotes the *cumulant* average of x^n. Hence, if we can determine the *analytic* form of $u(k)$ for large k, we can analytically continue to the imaginary axis and thereby obtain $[\tau^n]_{\rm av}$.

Analyzing the data in Fig. 13, we find that the first few cumulants of $f(x)$ are roughly of the form $(-0.13)^n$. If we use this form then

$$u(k) = \exp(-0.13ik) - 1 + 0.13ik, \tag{16}$$

which, from Eqs. (12) and (14), gives for $L \to \infty$

$$[\tau^n]_{\rm av} \sim \exp(1.13nz_0 \ln L) = L^{1.13nz_0}, \tag{17}$$

where we have used the fit in Fig. 16. This corresponds to the "sharp cut-off" mentioned above, i.e. one has dynamical scaling (except that z_0 is different from z_n for $n > 0$). However, the data is not good enough to be able to make this analytic continuation with any confidence.

As a result of this analysis of the distribution of $\ln \tau$, we infer that the value of z for $q = 24$ found above from $[\tau]_{\mathrm{av}}$ (and from τ_L in Sec. IV A, see Fig. 7) *may* only represent an effective exponent, valid for fairly small sizes.

V. CONCLUSIONS

We have studied the dynamics of the q-state random bond Potts ferromagnet at the critical point in two-dimensions for $q = 3$ and $q = 24$. In both cases we find conventional dynamical scaling, and our results for the dynamical exponent are compatible with those of Ref. 16. However, for $q = 3$, we find that the reduced variance of the relaxation time τ tends to a finite value for large L, while for $q = 24$ it is the reduced variance of $\ln \tau$ which tends to a finite value. Equivalently, for $q = 24$ one can say that the reduced variance of the barrier heights is finite. We do not have an intuitive explanation for this difference in behavior between the two cases, but it may be related to the transition of the pure system being first order for $q = 24$ and second order for $q = 3$. It is currently unclear whether the scaling of the distribution of barrier heights for $q = 24$ implies that dynamical scaling is actually activated for $L \to \infty$, in which case our finite value of z would just be an effective exponent valid for rather small sizes.

Acknowledgments

We acknowledge support from the NSF through grant DMR 0086287. We would like to thank Terry Olson for helpful discussions and for making available his code for the Wolff algorithm. One of us (APY) would also like to thank John Cardy for helpful discussions and comments on an early version of the manuscript. The other (CD) would like to thank UCSC for hospitality while part of this work was performed.

---

* Electronic address: `derouler@mozart.ucsc.edu`
† Electronic address: `peter@bartok.ucsc.edu`
[1] For a review of the Potts model, see F. Y. Wu, Rev. Mod. Phys. **54**, 235 (1982).
[2] Y. Imry and M. Wortis, Phys. Rev. B **19**, 3580 (1979).
[3] M. Aizenman and J. Wehr, Phys. Rev. Lett. **62**, 2503 (1989).
[4] K. Hui and A. N. Berker, Phys. Rev. Lett. **62**, 2507 (1989).
[5] A. W. W. Ludwig, Nucl. Phys. B, **330**, 639 (1990).
[6] J. Cardy and J. J. Jacobsen, Phys. Rev. Lett. **79**, 4063 (1997).
[7] J. J. Jacobsen and J. Cardy, Nucl. Phys. B, **515**, 701 (1998).
[8] T. Olson and A. P. Young, Phys. Rev. B **60**, 3428, (1999).
[9] C. Chatelain and B. Berche, Phys. Rev. Lett. **80**, 1670 (1998).
[10] C. Chatelain and B. Berche, Phys. Rev. E **58**, R6899 (1998).
[11] C. Chatelain and B. Berche, Phys. Rev. E **60**, 3853 (1999).
[12] C. Chatelain, B. Berche and L. N. Schur, cond-mat/0108014.
[13] M. Picco, Phys. Rev. Lett. **79** 2998 (1997).
[14] M. Picco, cond-mat/9802092
[15] H.-P. Ying and K. Haraga, Phys. Rev. E **62**, 174 (2000), (cond-mat/0001284).
[16] Z. Q. Pan, H.-P. Ying, and D. W. Gu, cond-mat/0103130.
[17] H.-P. Ying, B. J. Bian, D. R. Ji, H. J. Luo, and L. Schuelke, cond-mat/0103355.
[18] J. Cardy, Physica A, **263**, 215 (1999) (cond-mat/9806355).
[19] D. S. Fisher, Phys. Rev. Lett. **56**, 416 (1986).
[20] A. Aharony and A. B. Harris, Phys. Rev. Lett. **77**, 3700 (1996).
[21] A. Aharony, A. B. Harris and S. Wiseman, Phys. Rev. Lett. **81**, 252 (1998).
[22] S. Wiseman and E. Domany, Phys. Rev. E. **58**, 2938 (1998).
[23] W. Kinzel and E. Domany, Phys. Rev. B **23** 3421 (1981).
[24] In the published version, Ref. 8, the space between the factor $2/\pi$ and the rest of the expression in Eq. (3) is mysteriously missing, though the space was present in the version submitted to the journal, see cond-mat/9903068. According to this typo, π would only multiply the factor of $(1-x)^2$ in the denominator, which is incorrect.
[25] R. H. Swendsen and J. Wang, Phys. Rev. Lett. **58**, 86 (1987).
[26] U. Wolff, Phys. Rev. Lett. **62**, 361 (1989)
[27] B. E. Özoğuz, Y. Gündüç, and M. Aydin, Int. J. Mod. Phys. C **11**, 553 (2000).
[28] E. Buffenoir and S. Wallon, J. Phys. A. **26**, 3045 (1993).